

Bianisotropic Photonic Metamaterials

Christine Éliane Kriegler, Michael Stefan Rill, Stefan Linden, and Martin Wegener

(Invited Paper)

Abstract—In metamaterials, electric (magnetic) dipoles can be excited by the electric (magnetic) component of the incident light field. Moreover, in the description of bianisotropic metamaterials, cross terms occur, i.e., magnetic dipoles can also be excited by the electric-field component of the incident light and vice versa. For the cross terms, in the general bianisotropic case, the exciting field and dipole vectors include an arbitrary angle. For the special case of chirality, the angle is zero. In the spirit of a brief tutorial, a very simple electric-circuit description of the split-ring resonator is used to give a basic introduction to the cross terms. Mathematical details of the effective parameter retrieval are presented. Furthermore, we briefly review recent experiments on bianisotropic metamaterials operating at optical frequencies.

Index Terms—Bianisotropy, metamaterial, split-ring resonator.

I. INTRODUCTION

OPTICS has traditionally mainly dealt with dielectric materials. Here, the incident electric-field vector of the light excites microscopic electric dipoles that re-emit electromagnetic waves just like a dipole radio antenna. Other dipoles are excited by this re-emission and so on. This successive excitation and re-emission clearly modifies the phase velocity of light and determines the optical properties of the material, in particular its electric permittivity ϵ (or dielectric function).

One of the little revolutions in optics that the concept of artificial effective materials (“metamaterials”) has brought about is the fact that, similarly, magnetic dipoles can be excited by the magnetic-field component of the light, which can be cast into the effective magnetic permeability μ of the material [1]–[8] (or, alternatively, into spatial dispersion). The interplay of ϵ and μ has given rise to interesting new aspects of electromagnetism that have been reviewed several times [9]–[13], and will not be repeated here. In general, both ϵ and μ are tensors, i.e., the dipole direction is not necessarily identical to the exciting vector direction.

A further set of new possibilities originates from the “cross terms.” This means that, in general, magnetic dipoles can not only be excited by the magnetic field but also by the electric field. Similarly, electric dipoles can not only be excited by the electric field but also by the magnetic field. These cross terms are subject of the present review or brief tutorial. We focus on the

special case that the dipole vectors are oriented *perpendicular* to the exciting fields. If the dipole vectors are oriented *parallel* to the exciting fields, another special case arises, namely chirality.

Bianisotropy and chirality are very well-established parts of electromagnetism and a bulk of corresponding theoretical literature does exist [14]–[31]. Yet, based on our own experience, some of that literature is somewhat difficult to digest for an experimentalist. Thus, we start with a simple and intuitive tutorial based on an example, namely on split-ring resonators (SRRs). The discussion aims at giving an understanding and explaining the physics rather than a complete and/or a quantitative description. Next, we derive in detail the formulae required for retrieving the effective parameters of bianisotropic metamaterials from transmittance and reflectance data. Finally, we briefly review recent experiments on bianisotropic metamaterials operating at optical frequencies.

II. BIANISOTROPY

A. Split-Ring Resonators

An SRR is a metallic ring with one or several slits [1]–[8], [32]–[34] (see Fig. 1). The incident light field can induce a circulating and oscillating electric current in the metallic wire that gives rise to a local magnetic field (magnetic dipole) normal to the SRR plane. The resonance of the SRR can be thought of as arising from the inductance of an almost closed loop (inductance L) and the capacitor formed by the two ends of the wire (capacitance C). This leads to an LC eigenfrequency $\omega_{LC} = 1/\sqrt{LC}$. For small SRR, the kinetic inductance can add to L [35], [36]. Also, a more detailed modeling would have to account for additional surface contributions to the SRR capacitance C [37], [38]. Furthermore, energy can either be dissipated by Ohmic losses or can be radiated into free space, leading to the radiation resistance [39]–[41]. The effect of both can be lumped into an effective resistance R of the circuit.

Using Kirchhoff’s voltage law, the equation of motion of the electric current I in this simple circuit results as

$$U_C + U_R + U_L = \frac{1}{C} \int I dt + RI + L \frac{dI}{dt} = U_{\text{ind}}. \quad (1)$$

The incident light field induces the source voltage U_{ind} .

The SRR generally has both an electric and a magnetic dipole moment. As usual, the electric dipole moment is given by the charges separated on the capacitor plates, $\int I dt$, times their distance d . The macroscopic electric polarization P is the product of the individual electric dipole moment times the number density of the dipoles $N_{LC}/V = 1/(a_{xy}^2 a_z)$, where a_{xy} and a_z are the in-plane and out-of-plane lattice constants of the crystal composed of SRR—provided that we neglect interaction effects

Manuscript received March 6, 2009. First published June 16, 2009; current version published April 7, 2010.

The authors are with the Institut für Angewandte Physik and the DFG-Center for Functional Nanostructures (CFN), Universität Karlsruhe (TH), D-76131 Karlsruhe, Germany. They are also with the Institut für Nanotechnologie, Forschungszentrum Karlsruhe in der Helmholtz-Gemeinschaft, D-76021 Karlsruhe, Germany (e-mail: christine.kriegler@physik.uni-karlsruhe.de; michael.rill@physik.uni-karlsruhe.de; stefan.linden@physik.uni-karlsruhe.de; martin.wegener@physik.uni-karlsruhe.de).

Digital Object Identifier 10.1109/JSTQE.2009.2020809

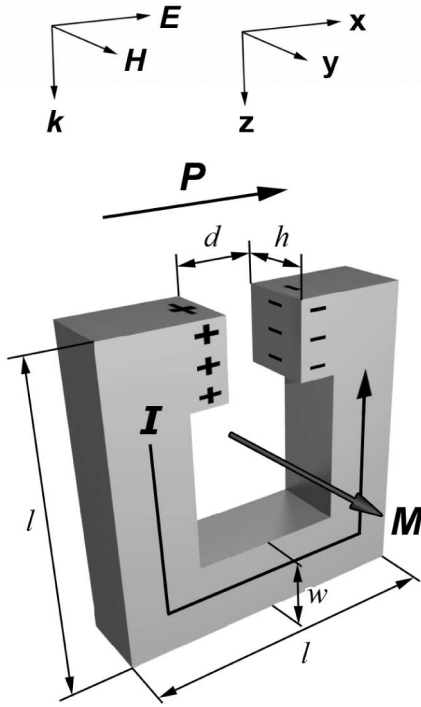


Fig. 1. Illustration of a split-ring resonator and the parameters used in the calculations. The excitation geometry considered in this section is also depicted.

among the SRR in the crystal. This leads to

$$P_x(t) = \frac{1}{a_{xy}^2 a_z} d \int I dt. \quad (2)$$

Similarly, the magnetic dipole density M is the product of the SRR number density and the individual magnetic dipole moment. Within the quasi-static limit (no retardation), the latter is given by the current I times the area of the loop. This leads to

$$M_y(t) = \frac{1}{a_{xy}^2 a_z} I(t) l^2. \quad (3)$$

Note that we have tacitly neglected the displacement current at this point. Hence, our reasoning is only strictly valid provided that the Ohmic current dominates over the displacement current (i.e., the slit in the SRR must not be too large).

- 1) Let us start by discussing a current that is solely induced by Faraday's induction law. In this case, we have $U_{\text{ind}}(t) = -\frac{\partial \phi}{\partial t}$ with the magnetic flux $\phi(t)$ given by $\phi(t) = \mu_0 H_y(t) l^2$. Assuming a harmonically varying magnetic field $H_y(t) = H_y \exp(-i\omega t) + \text{c.c.}$, we obtain $M_y(t) = M_y \exp(-i\omega t) + \text{c.c.}$ with

$$M_y = \frac{\mathcal{F} \omega^2}{\omega_{LC}^2 - \omega^2 - i\gamma\omega} H_y. \quad (4)$$

Here, we have employed the inductance of a long coil $L = \mu_0 l^2 / h$ and have introduced two abbreviations: the damping $\gamma = R/L$ and the SRR volume filling fraction $0 \leq \mathcal{F} \leq 1$ with

$$\mathcal{F} = \frac{l^2 h}{(a_{xy}^2 a_z)}. \quad (5)$$

Notably, induction via Faraday's law also leads to a polarization $P_x(t) = P_x \exp(-i\omega t) + \text{c.c.}$ with

$$P_x = \frac{d}{l^2} \frac{i\mathcal{F}\omega}{\omega_{LC}^2 - \omega^2 - i\gamma\omega} H_y. \quad (6)$$

Here, we have employed the capacitance $C = \epsilon_0 wh/d$ for a plate capacitor with large plates. Note that \vec{P} is phase delayed by 90° with respect to the exciting H -field. Otherwise it reveals the same resonance behavior around the LC eigenfrequency as the magnetization \vec{M} . Also note that the induced polarization goes to zero as the slit width d of the SRR is made smaller and smaller.

- 2) Next, we discuss a current that is induced by a voltage drop over the plate capacitor that arises from the electric-field component, $E_x(t)$, of the light field. In this case, we have $U_{\text{ind}}(t) = E_x(t) d$. Assuming a harmonically varying electric field $E_x(t) = E_x \exp(-i\omega t) + \text{c.c.}$, we obtain

$$M_y = \frac{1}{\mu_0} \frac{d}{l^2} \frac{-i\mathcal{F}\omega}{\omega_{LC}^2 - \omega^2 - i\gamma\omega} E_x \quad (7)$$

and

$$P_x = \frac{1}{\mu_0} \left(\frac{d}{l^2} \right)^2 \frac{\mathcal{F}}{\omega_{LC}^2 - \omega^2 - i\gamma\omega} E_x. \quad (8)$$

In this case, the 90° phase delay (see imaginary unit in numerator) occurs for the magnetization M_y .

Provided the displacement current is negligible [27] (which is usually fulfilled in the vicinity of the resonance), we can identify the macroscopic magnetization with the magnetic dipole density \vec{M} discussed above. Hence, we get the macroscopic material equations

$$\vec{D} = \epsilon_0 \vec{E} + \vec{P} \quad (9)$$

and

$$\vec{B} = \mu_0 (\vec{H} + \vec{M}). \quad (10)$$

We can summarize our findings in 1) and 2) for the SRR by

$$\begin{pmatrix} D_x \\ B_y \end{pmatrix} = \begin{pmatrix} \epsilon_0 \epsilon & -i\epsilon_0^{-1} \xi \\ +i\epsilon_0^{-1} \xi & \mu_0 \mu \end{pmatrix} \begin{pmatrix} E_x \\ H_y \end{pmatrix}. \quad (11)$$

Here, we have introduced the (dimensionless) electric permittivity

$$\epsilon(\omega) = 1 + \left(\frac{d c_0}{l^2} \right)^2 \frac{\mathcal{F}}{\omega_{LC}^2 - \omega^2 - i\gamma\omega} \quad (12)$$

the (dimensionless) magnetic permeability

$$\mu(\omega) = 1 + \frac{\mathcal{F} \omega^2}{\omega_{LC}^2 - \omega^2 - i\gamma\omega} \quad (13)$$

the (dimensionless) bianisotropy parameter

$$\xi(\omega) = -\frac{d c_0}{l^2} \frac{\mathcal{F} \omega}{\omega_{LC}^2 - \omega^2 - i\gamma\omega} \quad (14)$$

and the vacuum speed of light $c_0 = 1/\sqrt{\epsilon_0 \mu_0}$. ϵ describes the excitation of electric dipoles by the electric field of the light, μ the excitation of magnetic dipoles by the magnetic field, and ξ

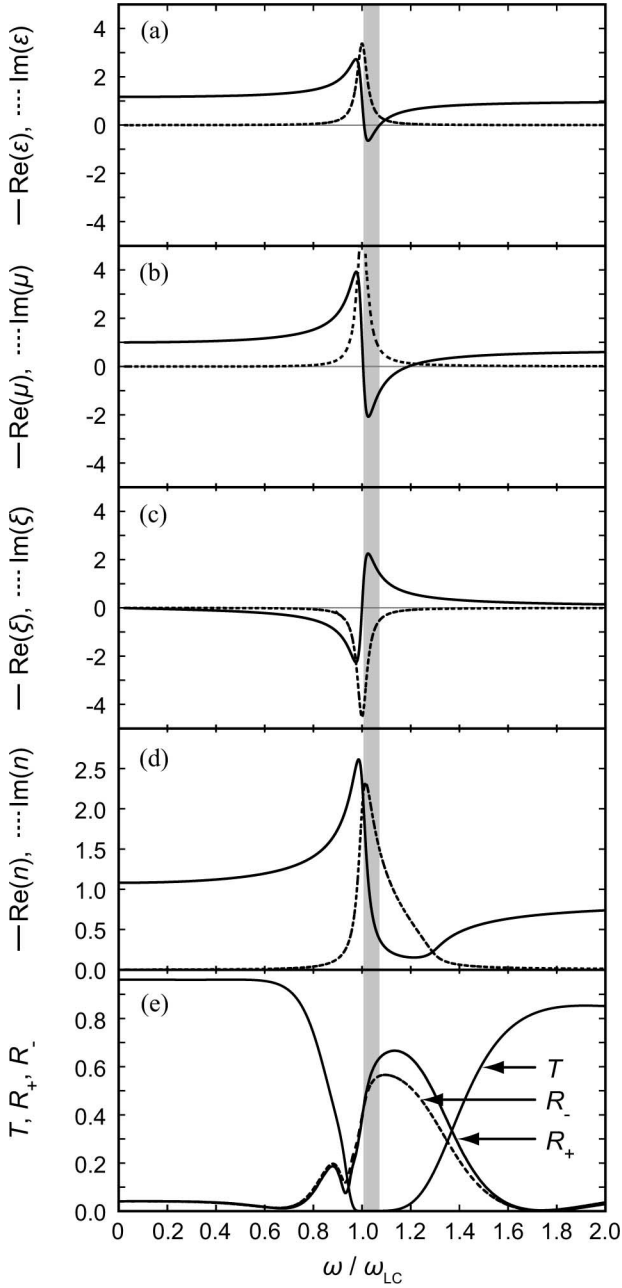


Fig. 2. (a) Electric permittivity ϵ , (b) magnetic permeability μ , (c) bianisotropy parameter ξ , and (d) refractive index n with $n^2 = \epsilon\mu - \xi^2$ versus normalized angular frequency ω/ω_{LC} for the split-ring resonator model described in this section (for geometry see Fig. 1). Real (imaginary) parts of these complex quantities are solid (dashed). Parameters are $\gamma/\omega_{LC} = 0.05$, $\mathcal{F} = 0.3$, and $dc_0/l^2 = 0.75 \times \omega_{LC}$. Note that the combination of $\text{Re}(\epsilon) < 0$ and $\text{Re}(\mu) < 0$ does *not* lead to $\text{Re}(n) < 0$ (not even if $\gamma/\omega_{LC} = 0$). (e) Normal-incidence intensity transmittance $T = T_+ = T_-$ and reflectances R_+ (light impinging from the left) and R_- (light impinging from the right) for a slab of material with parameters as in (a)–(d). Slab thickness is $c_0\pi/\omega_{LC}$ (half of a free-space LC eigenwavelength).

the excitation of magnetic dipoles by the electric field and vice versa. Fig. 2(a)–(d) illustrates these quantities.

If the slit in the SRR in Fig. 1 is at the lower part rather than at the top, the current induced by the electric field flows into the other direction and $+\xi \rightarrow -\xi$ (whereas $+\epsilon \rightarrow +\epsilon$ and $+\mu \rightarrow +\mu$).

Clearly, for the excitation geometry considered in Fig. 1, the single-slit SRR has no center of inversion along the propagation direction of light. If we introduce a second slit at the bottom of the SRR (i.e., opposite to the first slit), inversion symmetry is recovered. Provided we neglect retardation effects, the voltage drop over the second slit induced by the electric field is opposite in sign to that of the first slit, i.e., $I = 0$. Thus, neither magnetization nor polarization is induced by the electric field. A magnetic field component normal to the SRR plane can still induce a circulating and oscillating current, leading to a magnetic dipole moment. However, the electric dipole moment of the second slit is opposite to that of the first slit. Hence, no electric polarization results from the magnetic field of the incident light. Indeed, it is straightforward to show within our model that—under these conditions—the bianisotropy parameter ξ is strictly zero and $\epsilon = 1$, while $\mu \neq 1$. This finding, i.e., that a nonzero bianisotropy parameter requires breaking of inversion symmetry, is also valid beyond our simple SRR example.

B. Bianisotropic Parameter Retrieval

Light impinging under normal incidence onto such a slab of effective bianisotropic material will be partially reflected and partially transmitted according to the generalized version of the Fresnel equations. Owing to the lack of inversion symmetry, the reflectance does depend on from which side of the slab light impinges. In contrast, due to reciprocity, the transmittance does *not* depend on from which side light impinges. The dependence of the complex field transmittance and the two complex field reflectances on ϵ , μ , and ξ can be inverted, which forms an important ingredient for retrieving these effective parameters from numerical calculations and/or from experimental data. We have previously published the closed formulae for this retrieval for normal incidence of light in [42] (also see [19], [23]). In this section, we present the (somewhat lengthy) derivation that we have not published previously. These formulae are important when actually working with bianisotropy.

We consider a monochromatic, linearly polarized field $\vec{E}^i = E_x^i e^{i(k_1 z - \omega t)} \vec{e}_x$ and $\vec{H}^i = H_y^i e^{i(k_1 z - \omega t)} \vec{e}_y$, which impinges under normal incidence from an isotropic material of relative impedance z_1 (e.g., air or vacuum) onto a bianisotropic metamaterial slab of thickness d_s and which is transmitted into another isotropic material of relative impedance z_2 (e.g., a glass substrate). The geometry and the nomenclature used are illustrated in Fig. 3.

Considering the constitutive relations of the bianisotropic material (11) and introducing the following plane-wave ansatz $\vec{E}^\pm = E^\pm e^{i(k_\pm z - \omega t)} \vec{e}_x$ and $\vec{H}^\pm = H^\pm e^{i(k_\pm z - \omega t)} \vec{e}_y$ for both propagation directions (\pm) into Maxwell's equations immediately leads to eigensolutions. This means that no cross-polarization is excited as long as the wave propagates along this axis. A change in polarization could occur for oblique incidence of light onto the slab and/or for chiral media (see Section III). The corresponding dispersion relation reads $k_\pm = \pm n k_0$, where $k_0 = \omega c_0^{-1}$ is the vacuum wave vector. The refractive index n is

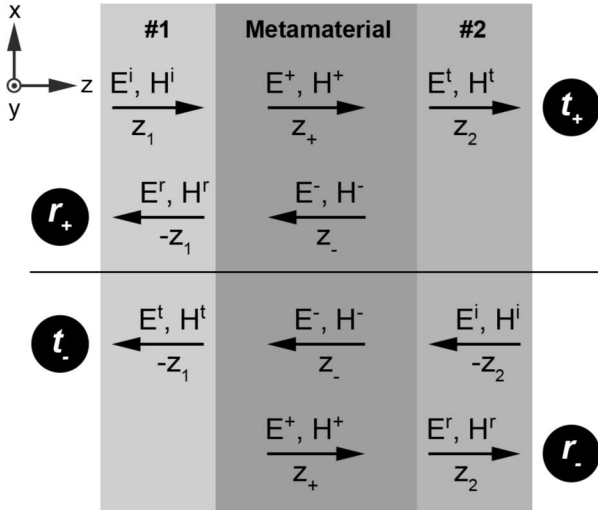


Fig. 3. Illustration of field components for the generalized version of Fresnel's equations for retrieving effective parameters including bianisotropy. The metamaterial of interest is clad between an isotropic material #1 (e.g., air) and another isotropic material #2 (e.g., a glass substrate). A substrate occurs in most metamaterial experiments at optical frequencies.

given by

$$n^2 = \epsilon\mu - \xi^2. \quad (15)$$

For a passive material, the root has to be chosen such that $\text{Im}(n) \geq 0$. Otherwise, exponentially growing solutions occur, violating energy conservation.

The bulk impedance of the bianisotropic material is Z_+ for propagation in the (+)-direction and $-Z_-$ for propagation in the (-)-direction. These quantities are given by $Z_+ = E^+/H^+$ and $Z_- = E^-/H^-$. We derive from Maxwell's equations

$$z_{\pm} \equiv Z_{\pm}/Z_0 = \mu(\pm n - i\xi)^{-1} \quad (16)$$

where $Z_0 = \sqrt{\mu_0/\epsilon_0}$ is the vacuum impedance. We note that $z_+ \neq -z_-$.

Using the boundary condition that the tangential components E and H are continuous and the fact that $HZ_0 = E/z_i$ and writing the complex reflectance and transmittance for a wave incident in the (+)-direction as $r_+ = E^r/E^i$ and $t_+ = E^t/E^i$, we get the following equations at $z = 0$:

$$(1 + r_+)E^i = E^+ + E^- \quad (17)$$

$$(1 - r_+)E^i/z_1 = E^+/z_+ + E^-/z_- \quad (18)$$

and at $z = d_s$:

$$E^+ e^{ink_0 d_s} + E^- e^{-ink_0 d_s} = t_+ E^i \quad (19)$$

$$E^+ e^{ink_0 d_s}/z_+ + E^- e^{-ink_0 d_s}/z_- = t_+ E^i/z_2. \quad (20)$$

With (17) and (18) [respectively, (19) and (20)] we express E^+/E^i and E^-/E^i as linear functions of r_+ (respectively t_+):

$$E^+/E^i = a_+ + b_+ r_+ \text{ and } E^-/E^i = c_+ + d_+ t_+$$

$$E^-/E^i = a_- + b_- r_+ \text{ and } E^-/E^i = c_- + d_- t_+.$$

This yields two linear relationships between r_+ and t_+

$$t_+ = \alpha + \beta r_+ \text{ and} \quad (21)$$

$$t_+ = \gamma + \delta r_+ \quad (22)$$

where

$$\alpha = e^{ink_0 d_s} (1 - z_-/z_1) (1 - z_-/z_2)^{-1}$$

$$\beta = e^{ink_0 d_s} (1 + z_-/z_1) (1 - z_-/z_2)^{-1}$$

$$\gamma = e^{-ink_0 d_s} (1 - z_+/z_1) (1 - z_+/z_2)^{-1}$$

$$\delta = e^{-ink_0 d_s} (1 + z_+/z_1) (1 - z_+/z_2)^{-1}.$$

We want to deduce the three complex parameters ϵ , μ , and ξ , which depend directly on n , z_+ , and z_- , from the complex transmittance and reflectance of the material. Therefore, (21) and (22) alone are not sufficient to solve the problem and we need to consider the case of propagation in the (-)-direction, too. In this case, (17)–(20) take the same form as previously, except that we have to make the following substitutions (see Fig. 3)

$$\begin{array}{cccc} (+)\text{-direction:} & z_1 & z_2 & z_+ & z_- \\ & \downarrow & \downarrow & \downarrow & \downarrow \end{array}$$

$$(-)\text{-direction:} \quad -z_2 \quad -z_1 \quad z_- \quad z_+.$$

As a consequence, we obtain the following equations, corresponding to (21) and (22), for the (-)-direction

$$t_- = \alpha' + \beta' r_- \text{ and} \quad (23)$$

$$t_- = \gamma' + \delta' r_- \quad (24)$$

where

$$\alpha' = e^{ink_0 d_s} (1 + z_+/z_2) (1 + z_+/z_1)^{-1}$$

$$\beta' = e^{ink_0 d_s} (1 - z_+/z_2) (1 + z_+/z_1)^{-1}$$

$$\gamma' = e^{-ink_0 d_s} (1 + z_-/z_2) (1 + z_-/z_1)^{-1}$$

$$\delta' = e^{-ink_0 d_s} (1 - z_-/z_2) (1 + z_-/z_1)^{-1}.$$

We note that $t_+/z_2 = t_-/z_1$ (calculation not detailed here), which results in $T = T_+ = T_-$, i.e., the intensity transmittance T does not depend on from which side of the slab light impinges onto the slab.

We now need to invert (21)–(24) in order to calculate z_+ , z_- , and n for known t_+ , r_+ , t_- , and r_- . Multiplying (21) by (24) and (22) by (23) yields

$$t_+ t_- = \alpha\gamma' + \beta\gamma' r_+ + \alpha\delta' r_- + \beta\delta' r_+ r_- \text{ and} \quad (25)$$

$$t_+ t_- = \gamma\alpha' + \delta\alpha' r_+ + \gamma\beta' r_- + \delta\beta' r_+ r_- \quad (26)$$

with

$$\alpha\gamma' = \frac{(1 - z_-/z_1)(1 + z_-/z_2)}{(1 + z_-/z_1)(1 - z_-/z_2)}$$

$$\gamma\alpha' = \frac{(1 - z_+/z_1)(1 + z_+/z_2)}{(1 + z_+/z_1)(1 - z_+/z_2)}$$

$$\beta\gamma' = (1 + z_-/z_2)(1 - z_-/z_2)^{-1}$$

$$\delta\alpha' = (1 + z_+/z_2)(1 - z_+/z_2)^{-1}$$

$$\alpha\delta' = (1 - z_-/z_1)(1 + z_-/z_1)^{-1}$$

$$\gamma\beta' = (1 - z_+/z_1)(1 + z_+/z_1)^{-1}$$

$$\beta\delta' = 1$$

$$\delta\beta' = 1.$$

It follows that (25) and (26) are the same equation for z_+ and z_- . It can be rewritten as a second-degree polynomial equation for z_{\pm} : $az_{\pm}^2 + bz_{\pm} + c = 0$, which means that

$$z_{\pm} = (-b \mp \sqrt{b^2 - 4ac}) / (2a) \quad (27)$$

with

$$\begin{aligned} a &= t_+ t_- - (1 - r_+) (1 - r_-) \\ b &= (z_1 - z_2) (t_+ t_- + 1 - r_+ r_-) + (z_1 + z_2) (r_+ - r_-) \\ c &= z_1 z_2 [-t_+ t_- + (1 + r_+) (1 + r_-)] . \end{aligned}$$

Again assuming a passive medium, the sign in (27) must be chosen in order to have a positive real part of the medium impedance. We have already noted that z_+ is the relative impedance of the bianisotropic medium in the (+)-direction and z_- is the opposite of the relative impedance in the (-)-direction, which yields $\text{Re}(z_+) > 0$ and $\text{Re}(-z_-) > 0$.

To find the refractive index, we can rewrite (21) and (22) as

$$\begin{aligned} t_+ &= e^{in k_0 d_s} [1 + r_+ - (1 - r_+) z_- / z_1] (1 - z_- / z_2)^{-1} \\ t_+ &= e^{-in k_0 d_s} [1 + r_+ - (1 - r_+) z_+ / z_1] (1 - z_+ / z_2)^{-1} . \end{aligned}$$

Finally, we get an implicit expression for the (complex) refractive index n

$$\cos(nk_0 d_s) = \frac{t_+}{2} \left[\frac{1 - z_- / z_2}{1 + r_+ - (1 - r_+) z_- / z_1} + \frac{1 - z_+ / z_2}{1 + r_+ - (1 - r_+) z_+ / z_1} \right] . \quad (28)$$

As usual, (28) has infinitely many solutions for n due to the different branches of the inverse cosine. To choose the correct one, we proceed as previously described for the parameter retrieval for structures with inversion symmetry [13].

Once z_{\pm} and n are at hand, we deduce ϵ , μ , and ξ from (27) and (28) via

$$\epsilon = (n + i\xi) / z_+ \quad (29)$$

$$\mu = (n - i\xi) z_+ \quad \text{and} \quad (30)$$

$$\xi = in(z_- + z_+) (z_- - z_+)^{-1} . \quad (31)$$

Let us illustrate this retrieval by the simple example shown in Fig. 4. The three dielectric layers shown there can be viewed as one ($N = 1$) unit cell of a periodic structure that has no center of inversion along the propagation direction of light (just like the SRR depicted in Fig. 1). Due to the broken inversion symmetry, the field reflectance clearly depends on from which side light impinges onto the stack under normal incidence. Applying the aforementioned bianisotropic retrieval to this case at, e.g., $\lambda = 1 \mu\text{m}$ ($\gg d_1 = d_2 = d_3 = 10 \text{ nm}$) wavelength leads to the effective parameters $\epsilon = 6.72$, $\mu = 1.00$, and $\xi = -0.21$ that refer to a fictitious single homogeneous effective slab with total thickness $d_s = d_1 + d_2 + d_3 = 30 \text{ nm}$. We have explicitly verified that the same parameters are retrieved if $N = 2, 3, 4, \dots, 20$ unit cells of the identical three-layer structure are considered (i.e., the total slab thickness is $N \times 30 \text{ nm}$). Thus, the retrieved

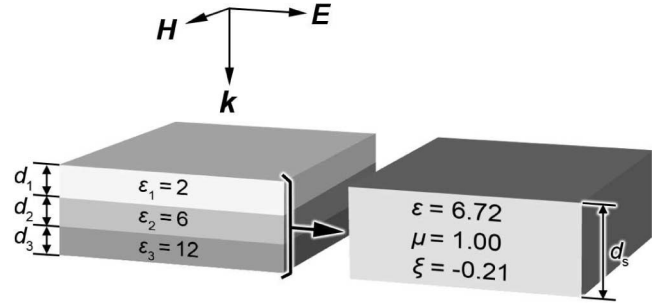


Fig. 4. Stack of three purely dielectric materials with (real) dielectric constants $\epsilon_1 = 2$, $\epsilon_2 = 6$, and $\epsilon_3 = 12$ and thicknesses $d_1 = d_2 = d_3 = 10 \text{ nm}$ embedded in vacuum breaks inversion symmetry. For example, at $1 \mu\text{m}$ free-space wavelength (300 THz frequency) and for normal-incidence of light, the physics can equivalently be described by a single effective 30-nm thin slab with permittivity $\epsilon = 6.72$, magnetic permeability $\mu = 1.00$, and bianisotropy parameter $\xi = -0.21$.

quantities ϵ , μ , and ξ can indeed be interpreted as effective material parameters. As the damping is strictly zero in this example, no absorption occurs. Hence, the sum of transmittance and reflectance is unity—for each propagation direction. Thus, the two intensity reflectances R_+ and R_- are identical in this case and differences occur only in the phases of the field reflectances r_+ and r_- .

This simple example clearly shows that one should be somewhat cautious with using the well-known Maxwell–Garnett approximation at this point, as it would cast the effective behavior of the three subwavelength dielectric layers in Fig. 4 into just an effective dielectric function

$$\epsilon = 1 + \frac{(\epsilon_1 - 1)d_1 + (\epsilon_2 - 1)d_2 + (\epsilon_3 - 1)d_3}{d_1 + d_2 + d_3} = 6.67 \quad (32)$$

assuming $\mu = 1$ and $\xi = 0$, leading to a single impedance $Z = \sqrt{\mu/\epsilon} \times Z_0$. The Maxwell–Garnett approximation obviously ignores that the field reflectance depends on from which side of the slab it is measured. This may or may not be important, depending on the problem.

C. Experiments

Experiments on bianisotropic metamaterials—including retrieval of the bianisotropy parameter—have been published for microwave [19], [23], [43], far-infrared [44], and optical frequencies [42], [45], [46]. Related structures have been fabricated previously [47], [48] but bianisotropy has not been mentioned. Fig. 5 shows electron micrographs of three different optical-regime samples that have been fabricated in our group by direct laser writing (see, e.g., review in [13]) of a polymeric template and subsequent metallization. Metallization is accomplished either by chemical vapor deposition of silver [42], [45] [Fig. 5(a), (c), and (d)] or by high-vacuum shadow evaporation of silver [46] [Fig. 5(b)]. The structures in Fig. 5(c) and (d) are derived from (a) via post-processing using focused-ion-beam (FIB) milling [45]. The structures in (a) and (b) have also been FIB cut to reveal their interior. Obviously, all four samples in Fig. 5 are variations of the SRR geometry shown in Fig. 1. In Fig. 5(a), the SRRs are connected in two directions, in (b) they

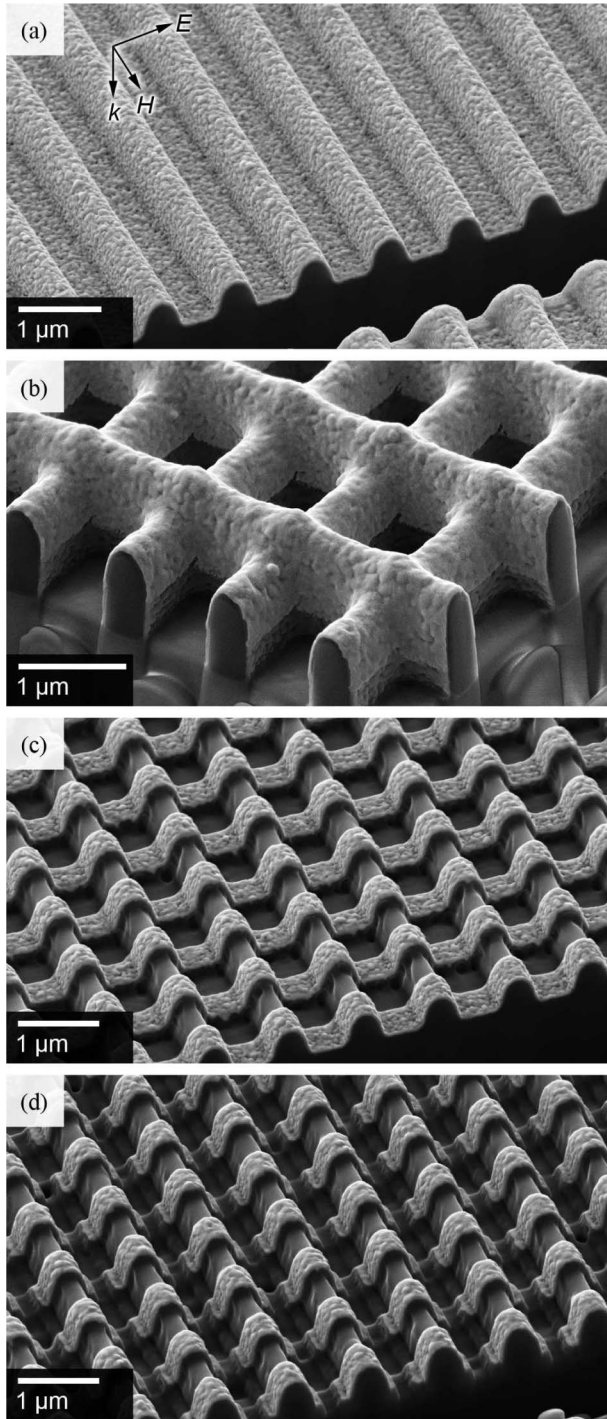


Fig. 5. Oblique-view electron micrographs of three different, though related, recently experimentally fabricated bianisotropic photonic metamaterials. (a) Taken from [45] (sample similar to but different from that in [42]), (b) taken from [46], and (c) as well as (d) taken from [45]. The dark parts correspond to the polymeric templates, light gray parts to the silver films.

are connected along one direction only and an additional orthogonal set of intentionally elevated metallic wires has been introduced. The corresponding increased design freedom has led to a negative phase velocity [46] (i.e., to $\text{Re}(n) < 0$). In (c), the SRRs are also only connected along one direction, whereas (d) is a 2-D array of disconnected SRR similar to Fig. 1.

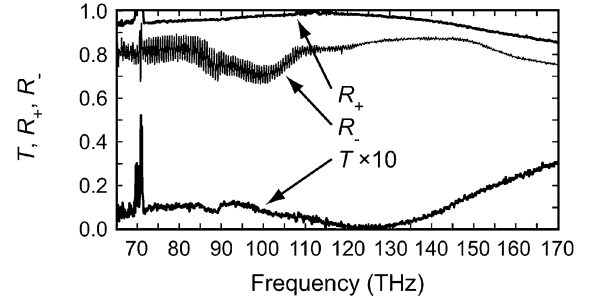


Fig. 6. Measured normal-incidence intensity transmittance (T) and reflectances (R_+ , R_-) corresponding to the calculated spectrum shown in Fig. 7(e). The polarization of the incident electromagnetic field is illustrated on the upper left-hand-side corner of Fig. 5(a). The rapid oscillations of R_- are due to Fabry-Perot interferences in the 170- μm -thick glass substrate. Artifacts at around 70 THz are caused by absorption lines of CO_2 .

As an example, Fig. 7(a)–(d) shows the results of the parameter retrieval (see previous section) for the structure corresponding to Fig. 5(a), the measured intensity transmittance and reflectance spectra of which are depicted in Fig. 6. For computational details see [45]. This structure is an improved version [45] of the one published in [42]. Again [compare Fig. 2(a)], the real part of the refractive index is positive ($\text{Re}(n) > 0$) despite the fact that both $\text{Re}(\epsilon) < 0$ and, at the same time, $\text{Re}(\mu) < 0$ due to the very significant influence of the bianisotropy parameter ξ . The fact that $\xi \neq 0$ in Fig. 7(c) is intimately connected to $R_+ \neq R_-$ in Fig. 7(e).

III. CHIRALITY

In Section II and in particular in (11), we have used a scalar formulation for ξ and the other quantities (ϵ and μ). Equation (11) has been a special example of the more general form for reciprocal media

$$\begin{pmatrix} \vec{D} \\ \vec{B} \end{pmatrix} = \begin{pmatrix} \epsilon_0 \underline{\epsilon} & -ic_0^{-1} \underline{\xi} \\ +ic_0^{-1} \underline{\xi}^t & \mu_0 \underline{\mu} \end{pmatrix} \begin{pmatrix} \vec{E} \\ \vec{H} \end{pmatrix} \quad (33)$$

where $\underline{\epsilon}$, $\underline{\mu}$, and $\underline{\xi}$ are tensors. $\underline{\xi}^t$ is the transposed of $\underline{\xi}$. In this general bianisotropic case, regarding the cross terms, the electric polarization is no longer necessarily perpendicular to the exciting magnetic-field vector and, similarly, the magnetization is no longer necessarily perpendicular to the exciting electric-field vector.

Another special example of the general bianisotropic case (33) is

$$\begin{pmatrix} \vec{D} \\ \vec{B} \end{pmatrix} = \begin{pmatrix} \epsilon_0 \epsilon & -ic_0^{-1} \xi \\ +ic_0^{-1} \xi & \mu_0 \mu \end{pmatrix} \begin{pmatrix} \vec{E} \\ \vec{H} \end{pmatrix} \quad (34)$$

where ϵ , μ , and ξ are again scalars. Note that (34) looks rather similar to (11) at first sight. However, it has a totally different meaning and leads to completely different behavior, namely to chirality. Chiral metamaterials are a subclass of bianisotropic metamaterials. Let us briefly elaborate on the differences with respect to the previous section.

For a plane wave propagating through a medium, the incident electric and magnetic vector components are perpendicular to

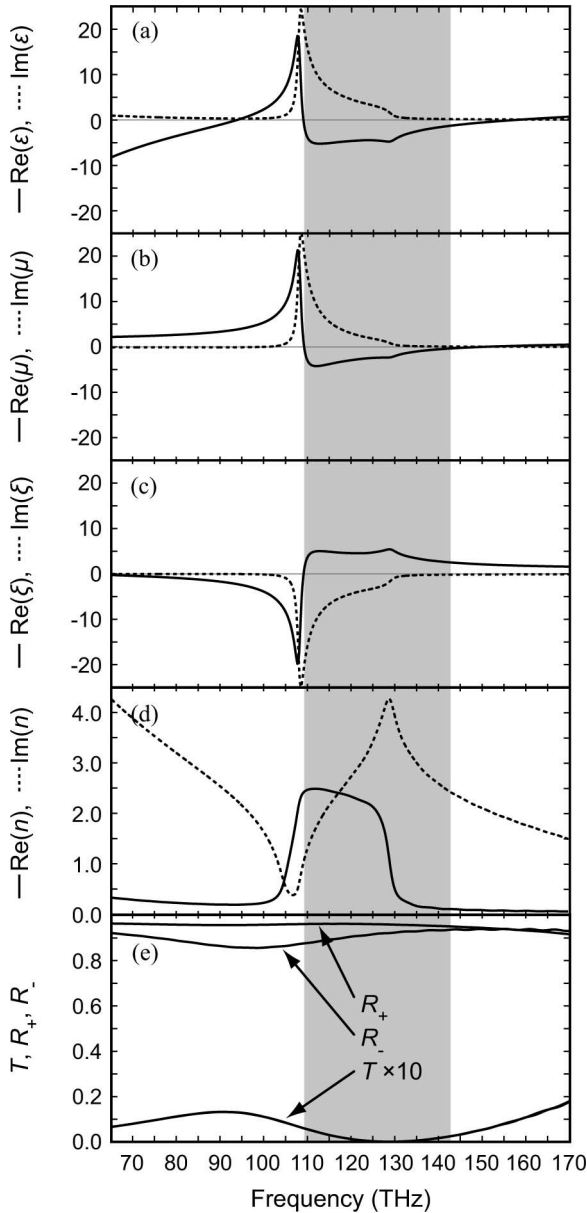


Fig. 7. (a)–(d) Retrieved effective parameters from numerical calculation of the complex transmittance and reflectances of the structure shown in Fig. 5 (a). (e) Calculated normal-incidence intensity transmittance (T) and reflectances (R_+ , R_-) of this structure.

each other. If, as the wave passes through the chiral medium following (34), the magnetic component induces an electric dipole *parallel* to the magnetic field vector, the resulting net local electric field vector will clearly be rotated a bit. Likewise, magnetic dipoles are excited by the electric vector component. Hence, the magnetic field vector rotates as well—regardless of the incident polarization of light. Thus, the eigenstates no longer correspond to linear polarization of light (as in the preceding section) but rather to circular polarization of light. On the basis of this, the refractive index can be expressed [49] via

$$n_{\pm} = \sqrt{\epsilon\mu} \mp \xi. \quad (35)$$

As usual, the sign of the complex root has to be chosen appropriately. The other signs in (35) refer to right-handed (+) and left-handed (−) circular polarization of light, respectively. The difference of the two refractive indices becomes $n_+ - n_- = -2\xi$. The behavior of (35) is very different from that for the other special case of bianisotropy in (15). For example, in principle, (35) allows for a negative index of refraction (precisely, a negative phase velocity of light) for one handedness of light if both ϵ and μ are mainly real and positive—if only the modulus of ξ is sufficiently large. In this sense, a large real value of ξ is helpful for pure chirality, whereas a large real value of ξ works against a negative phase velocity of light for pure bianisotropy, because a large ξ^2 in (15) leads to a negative n^2 , i.e., to evanescent waves.

Retrieval of the effective parameters of purely chiral metamaterials (the analogue of our discussion in Sect. II.B.) has been published [49]. First chiral negative-index metamaterials [50] have recently been realized at microwave [51] and far-infrared [52] frequencies.

IV. SUMMARY AND OUTLOOK

The advance of man-made metamaterials has significantly increased our possibilities regarding manipulating light via optical materials. Light is an electromagnetic wave with an electric and a magnetic vector component. Either of them can excite both electric and magnetic dipoles inside the material. These dipoles can be parallel or orthogonal to the exciting field component—leading to a rich variety of cases. If, for example, the magnetic (electric) dipoles excited by the electric (magnetic) field vector are perpendicular to each other, the reflectance of a slab of such material becomes asymmetric. A negative phase velocity of linearly polarized light (“negative-index metamaterials”) can still be achieved in this case, however bianisotropy is not usually helpful. In particular, the phase velocity of light can be positive even if both electric permittivity and magnetic permeability are negative. In contrast, if, for example, the magnetic (electric) dipoles excited by the electric (magnetic) field vector are parallel to each other, the medium becomes chiral. Chirality tends to enable negative phase velocities. In particular, for strong chirality, the phase velocity of circularly polarized light can be negative even if both permittivity and permeability are positive. At optical frequencies, special bianisotropic negative-index structures have been realized experimentally, while chiral negative-index structures have not. However, interesting and encouraging results have recently been published at Gigahertz (microwave) and Terahertz (far-infrared) frequencies. Results on chiral photonic metamaterials exhibiting a positive phase velocity of light have been published previously [53]–[58].

It is rather likely that chiral negative-index metamaterials operating at optical frequencies will be realized experimentally in the near future. However, all chiral photonic metamaterials presented so far are uniaxial and, hence, highly anisotropic. The design and experimental realization of isotropic chiral artificial materials operating at optical frequencies pose a major future challenge, especially regarding 3-D nanofabrication. For such materials, negative reflection of light has been predicted theoretically [30]. Finally, further possibilities arise if Faraday

active ingredients are incorporated into the metamaterial. In this case, not only the reflectance but also the transmittance can become asymmetric [22], [31], which might, e.g., give rise to very compact optical isolators.

ACKNOWLEDGMENT

The authors thank C. M. Soukoulis for discussions. They acknowledge financial support via the project PHOME of the Future and Emerging Technologies (FET) program within the Seventh Framework Programme for Research of the European Commission, under FET-Open grant number 213390 and via the METAMAT project by the Bundesministerium für Bildung und Forschung (BMBF). The authors further acknowledge support of the Deutsche Forschungsgemeinschaft (DFG) and the State of Baden–Württemberg through the DFG-Center for Functional Nanostructures (CFN) within subprojects A 1.4 and A 1.5. The research of S. Linden is further supported through a Helmholtz-Hochschul-Nachwuchsgruppe (VH-NG-232), the Ph.D. education of C. E. Kriegler and M. S. Rill by the Karlsruhe School of Optics and Photonics (KSOP). C. E. Kriegler is also supported by the Université de Bourgogne (Dijon, France).

REFERENCES

- [1] J. Pendry, A. Holden, D. Robbins, and W. Stewart, "Magnetism from conductors and enhanced nonlinear phenomena," *IEEE Trans. Microw. Theory Tech.*, vol. 47, no. 11, pp. 2075–2084, Nov. 1999.
- [2] D. Smith, W. Padilla, D. Vier, S. Nemat-Nasser, and S. Schultz, "Composite medium with simultaneously negative permeability and permittivity," *Phys. Rev. Lett.*, vol. 84, no. 18, pp. 4184–4187, 2000.
- [3] R. Shelby, D. Smith, and S. Schultz, "Experimental verification of a negative index of refraction," *Science*, vol. 292, pp. 77–79, 2001.
- [4] C. G. Parazzoli, R. B. Greggor, K. Li, B. E. C. Koltenbah, and M. Tanielian, "Experimental verification and simulation of negative index of refraction using Snell's law," *Phys. Rev. Lett.*, vol. 90, no. 10, pp. 107401-1–107401-4, 2003.
- [5] J. D. Baena, R. Marqués, F. Medina, and J. Martel, "Artificial magnetic metamaterial design by using spiral resonators," *Phys. Rev. B*, vol. 69, no. 1, pp. 014402-1–014402-5, 2004.
- [6] T. J. Yen, W. J. Padilla, N. Fang, D. C. Vier, D. R. Smith, J. B. Pendry, D. N. Basov, and X. Zhang, "Terahertz magnetic response from artificial materials," *Science*, vol. 303, no. 5663, pp. 1494–1496, 2004.
- [7] S. Linden, C. Enkrich, M. Wegener, J. Zhou, T. Koschny, and C. M. Soukoulis, "Magnetic response of metamaterials at 100 terahertz," *Science*, vol. 306, pp. 1351–1353, 2004.
- [8] W. Xu, L. W. Li, H. Y. Yao, T. S. Yeo, and Q. Wu, "Extraction of constitutive relation tensor parameters of SRR structures using transmission line theory," *J. Electromagn. Waves Appl.*, vol. 20, no. 1, pp. 13–25, 2006.
- [9] D. R. Smith, J. B. Pendry, and M. Wiltshire, "Metamaterials and negative refractive index," *Science*, vol. 305, pp. 788–792, 2004.
- [10] N. Engheta and R. W. Ziolkowski, Eds., *Metamaterials: Physics and Engineering Explorations*. New York: Wiley–Interscience, 2006.
- [11] V. M. Shalaev, "Optical negative-index metamaterials," *Nat. Photon.*, vol. 1, pp. 41–48, 2007.
- [12] C. M. Soukoulis, S. Linden, and M. Wegener, "Negative refractive index at optical wavelengths," *Science*, vol. 315, pp. 47–49, 2007.
- [13] K. Busch, G. von Freymann, S. Linden, S. Mingalae, L. Tkeshelashvili, and M. Wegener, "Periodic nanostructures for photonics," *Phys. Rep.*, vol. 444, no. 1, pp. 101–202, 2007.
- [14] L. Vegni and A. Toscano, "Radiation of an electric point-source in a homogeneous omega medium," *J. Franklin Inst.: Eng. Appl. Math.*, vol. 332B, no. 5, pp. 579–594, 1995.
- [15] A. Bungay, Y. Svirko, and N. Zheludev, "Equivalency of the Casimir and the Landau–Lifshitz approaches to continuous-media electrodynamics and optical activity on reflection," *Phys. Rev. B*, vol. 47, no. 18, pp. 11 730–11 735, 1993.
- [16] W. S. Weiglhofer, "On anomalous propagation in axially uniaxial bianisotropic mediums," *Int. J. Infrared Millim. Waves*, vol. 20, no. 7, pp. 1277–1286, 1999.
- [17] W. S. Weiglhofer, "On anomalous propagation in transversely uniaxial bianisotropic mediums," *Int. J. Infrared Millim. Waves*, vol. 21, no. 6, pp. 895–904, 2000.
- [18] A. Serdyukov, I. V. Semchenko, S. A. Tretyakov, and A. Sihvola, *Electromagnetics of Bi-Anisotropic Materials: Theory and Applications*. New York: Gordon and Breach, 2001.
- [19] R. Marqués, F. Medina, and R. Rafii-El-Idrissi, "Role of bianisotropy in negative permeability and left-handed metamaterials," *Phys. Rev. B*, vol. 65, no. 14, pp. 144440-1–144440-6, 2002.
- [20] S. Tretyakov, I. Nefedov, A. Sihvola, S. Maslovski, and C. Simovski, "Waves and energy in chiral nihility," *J. Electromagn. Waves Appl.*, vol. 17, no. 5, pp. 695–706, 2003.
- [21] J. B. Pendry, "A chiral route to negative refraction," *Science*, vol. 306, pp. 1353–1355, 2004.
- [22] T. G. Mackay and A. Lakhtakia, "Plane waves with negative phase velocity in Faraday chiral mediums," *Phys. Rev. E*, vol. 69, no. 2, pp. 026602-1–026602-9, 2004.
- [23] X. Chen, B.-I. Wu, J. A. Kong, and T. M. Grzegorzczak, "Retrieval of the effective constitutive parameters of bianisotropic metamaterials," *Phys. Rev. E*, vol. 71, no. 4, pp. 046610-1–046610-9, 2005.
- [24] Z. F. Li, K. Aydin, and E. Ozbay, "Determination of the effective constitutive parameters of bianisotropic metamaterials from reflection and transmission coefficients," *Phys. Rev. E*, vol. 79, no. 2, pp. 026610-1–026610-7, 2009.
- [25] T. M. Grzegorzczak, X. Chen, J. Pacheco, J. Chen, B. I. Wu, and J. A. Kong, "Reflection coefficients and Goos–Hänchen shifts in anisotropic and bianisotropic left-handed metamaterials," *Prog. Electromagn. Res., PIER*, vol. 51, pp. 83–113, 2005.
- [26] S. Tretyakov, A. Sihvola, and L. Jylhä, "Backward-wave regime and negative refraction in chiral composites," *Photon. Nanostruct.*, vol. 3, pp. 107–115, 2005.
- [27] V. M. Agranovich and Y. N. Gartstein, "Spatial dispersion and negative refraction of light," *Phys. Usp.*, vol. 49, pp. 1029–1044, 2006.
- [28] S. A. Tretyakov, C. R. Simovski, and M. Hudlicka, "Bianisotropic route to the realization and matching of backward-wave metamaterial slabs," *Phys. Rev. B*, vol. 75, pp. 153104-1–153104-4, 2007.
- [29] J. Kästel, M. Fleischhauer, S. Yelin, and R. Walsworth, "Tunable negative refraction without absorption via electromagnetically induced chirality," *Phys. Rev. Lett.*, vol. 99, no. 7, pp. 073602-1–073602-4, 2007.
- [30] C. Zhang and T. J. Cui, "Negative reflections of electromagnetic waves in a strong chiral medium," *Appl. Phys. Lett.*, vol. 91, pp. 194101-1–194101-3, 2007.
- [31] T. G. Mackay and A. Lakhtakia, "Negative reflection in a Faraday chiral medium," *Microw. Opt. Technol. Lett.*, vol. 50, no. 5, pp. 1368–1371, 2008.
- [32] H. J. Schneider and P. Dullenkopf, "Slotted tube resonator: A new NMR probe head at high observing frequencies," *Rev. Sci. Instrum.*, vol. 48, no. 1, pp. 68–73, 1977.
- [33] W. N. Hardy and L. A. Whitehead, "Split-ring resonator for use in magnetic-resonance from 200–2000 MHz," *Rev. Sci. Instrum.*, vol. 52, no. 2, pp. 213–216, 1981.
- [34] B. T. Ghim, G. A. Rinard, R. W. Quine, S. S. Eaton, and G. R. Eaton, "Design and fabrication of copper-film loop-gap resonators," *J. Magn. Res. A*, vol. 120, no. 1, pp. 72–76, 1996.
- [35] S. Linden, C. Enkrich, G. Dolling, M. W. Klein, J. Zhou, T. Koschny, C. M. Soukoulis, S. Burger, F. Schmidt, and M. Wegener, "Photonic metamaterials: Magnetism at optical frequencies," *IEEE J. Sel. Topics Quantum Electron.*, vol. 12, no. 6, pp. 1097–1105, Nov./Dec. 2006.
- [36] M. W. Klein, C. Enkrich, M. Wegener, C. M. Soukoulis, and S. Linden, "Single-slit split-ring resonators at optical frequencies: Limits of size scaling," *Opt. Lett.*, vol. 31, pp. 1259–1261, 2006.
- [37] L. Zhou and S. T. Chui, "Eigenmodes of metallic ring systems: A rigorous approach," *Phys. Rev. B*, vol. 74, no. 3, pp. 035419-1–035419-7, 2006.
- [38] O. Sydoruk, E. Tatartschuk, E. Shamonina, and L. Solymar, "Analytical formulation for the resonant frequency of split rings," *J. Appl. Phys.*, vol. 105, no. 1, pp. 014903-1–014903-4, 2009.
- [39] T. P. Meyrath, T. Zentgraf, and H. Giessen, "Lorentz model for metamaterials: Optical frequency resonance circuits," *Phys. Rev. B*, vol. 75, no. 20, pp. 205102-1–205102-5, 2007.
- [40] M. Husnik, M. W. Klein, N. Feth, M. König, J. Niegemann, K. Busch, S. Linden, and M. Wegener, "Absolute extinction cross-section of individual magnetic split-ring resonators," *Nat. Photon.*, vol. 2, pp. 614–617, 2008.
- [41] C. A. Balanis, *Antenna Theory: Analysis and Design*. New York: Harper & Row, 1982.

- [42] M. S. Rill, C. Plet, M. Thiel, I. Staude, G. von Freymann, S. Linden, and M. Wegener, "Photonic metamaterials by direct laser writing and silver chemical vapour deposition," *Nat. Mater.*, vol. 7, pp. 543–546, 2008.
- [43] D. R. Smith, J. Gollub, J. J. Mock, W. J. Padilla, and D. Schurig, "Calculation and measurement of bianisotropy in a split ring resonator metamaterial," *J. Appl. Phys.*, vol. 100, no. 2, pp. 024507-1–024507-9, 2006.
- [44] X. L. Xu, B. G. Quan, C. Z. Gu, and L. Wang, "Bianisotropic response of microfabricated metamaterials in the terahertz region," *J. Opt. Soc. Amer. B*, vol. 23, pp. 1174–1180, 2006.
- [45] C. E. Kriegler, M. S. Rill, M. Thiel, E. Müller, S. Essig, A. Frölich, G. von Freymann, S. Linden, D. Gerthsen, H. Hahn, K. Busch, and M. Wegener, "Transition between corrugated metal films and split-ring-resonator arrays," *Appl. Phys. B*, vol. 96, no. 4, pp. 749–755, 2009.
- [46] M. S. Rill, C. E. Kriegler, M. Thiel, G. von Freymann, S. Linden, and M. Wegener, "Negative-index bianisotropic photonic metamaterial fabricated by direct laser writing and silver shadow evaporation," *Opt. Lett.*, vol. 34, no. 1, pp. 19–21, 2009.
- [47] S. Zhang, W. Fang, B. K. Minhas, A. Frauenglass, K. J. Malloy, and S. R. J. Brueck, "Midinfrared resonant magnetic nanostructures exhibiting a negative permeability," *Phys. Rev. Lett.*, vol. 94, no. 3, pp. 037402-1–037402-4, 2005.
- [48] H. Schweizer, L. Fu, H. Gräbeldinger, H. Guo, N. Liu, S. Kaiser, and H. Giessen, "Midinfrared resonant magnetic nanostructures exhibiting a negative permeability," *Phys. Status Solidi A*, vol. 204, no. 11, pp. 3886–3900, 2007.
- [49] D. H. Kwon, D. H. Werner, A. V. Kildishev, and V. M. Shalaev, "Material parameter retrieval procedure for general bi-isotropic metamaterials and its application to optical chiral negative-index metamaterial design," *Opt. Exp.*, vol. 16, no. 16, pp. 11 822–11 829, 2008.
- [50] M. Wegener and S. Linden, "Giving light yet another new twist," *Physics*, vol. 2, p. 3, Jan. 2009.
- [51] E. Plum, J. Zhou, J. Dong, V. A. Fedotov, T. Koschny, C. M. Soukoulis, and N. I. Zheludev, "Metamaterial with negative index due to chirality," *Phys. Rev. B*, vol. 79, no. 3, pp. 035407-1–035407-6, 2009.
- [52] S. Zhang, Y.-S. Park, J. Li, X. Lu, W. Zhang, and X. Zhang, "Negative refractive index in chiral metamaterials," *Phys. Rev. Lett.*, vol. 102, no. 2, pp. 023901-1–023901-4, 2009.
- [53] Y. Svirko, N. Zheludev, and M. Osipov, "Layered chiral metallic microstructures with inductive coupling," *Appl. Phys. Lett.*, vol. 78, no. 4, pp. 498–500, 2001.
- [54] A. S. Schwanecke, A. Krasavin, D. M. Bagnall, A. Potts, A. V. Zayats, and N. I. Zheludev, "Broken time reversal of light interaction with planar chiral nanostructures," *Phys. Rev. Lett.*, vol. 91, no. 24, pp. 247404-1–247404-4, 2003.
- [55] M. Kuwata-Gonokami, N. Saito, Y. Ino, M. Kauranen, K. Jefimovs, T. Vallius, J. Turunen, and Y. Svirko, "Giant optical activity in quasi-two-dimensional planar nanostructures," *Phys. Rev. Lett.*, vol. 95, no. 22, pp. 227401-1–227401-4, 2005.
- [56] A. V. Rogacheva, V. A. Fedotov, A. S. Schwanecke, and N. I. Zheludev, "Giant gyrotropy due to electromagnetic-field coupling in a bilayered chiral structure," *Phys. Rev. Lett.*, vol. 97, no. 17, pp. 1177401-1–1177401-4, 2006.
- [57] F. Miyamaru and M. Hangyo, "Strong optical activity in chiral metamaterials of metal screw hole arrays," *Appl. Phys. Lett.*, vol. 89, no. 21, pp. 211105-1–211105-3, 2006.
- [58] M. Decker, M. W. Klein, M. Wegener, and S. Linden, "Circular dichroism of planar chiral magnetic metamaterials," *Opt. Lett.*, vol. 32, no. 7, pp. 856–858, 2007.



Christine Éliane Kriegler received the Master's degree in physics from the École Normale Supérieure de Lyon, Lyon, France, and the Diploma in physics from the Universität Karlsruhe (TH), Karlsruhe, Germany, in 2008. She is currently working toward the Ph.D. degree in physics at the Université de Bourgogne, Dijon, France, and the Universität Karlsruhe (TH).

During 2005 and 2006, she was an Intern with the European Molecular Biology Laboratory, Heidelberg, Germany, where she was engaged in research on molecular motors, and at the École Centrale de Lyon, where she worked in hydrodynamics. She received the "Agrégation de physique" in 2007. Her current research interests include the design, fabrication, and characterization of 3-D metallic nanostructures.



Michael Stefan Rill received the Diploma in physics from the Universität Ulm, Ulm, Germany, in 2006. He is currently working toward the Ph.D. degree in physics at the Universität Karlsruhe (TH), Karlsruhe, Germany.

He was engaged in the field of X-ray dosimetry. His current research interests include the fabrication and characterization of 3-D photonic metamaterials at optical frequencies.



Stefan Linden received the Ph.D. degree from Philipps-Universität Marburg, Marburg, Germany, in 2002.

He is currently the Head of a Helmholtz-Hochschul-Nachwuchgruppe, Institut für Nanotechnologie, Forschungszentrum Karlsruhe GmbH. From 2002 to 2003, he was a Postdoctoral Researcher at the University of Toronto, Toronto, ON, Canada and joint Prof. Martin Wegener's group at the Institut für Angewandte Physik, Universität Karlsruhe (TH), Karlsruhe, Germany in 2003.

Dr. Linden received the Heinz Mayer Leibniz-Award of the Deutsche Forschungsgemeinschaft (DFG) in 2007 for his research on photonic metamaterials.



Martin Wegener received the Ph.D. degree from the Physics Department, Johann Wolfgang Goethe-Universität Frankfurt, Frankfurt, Germany, in 1987.

He was a Postdoctoral Researcher at AT&T Bell Laboratories, Holmdel, NJ. In June 1990, he became an Associate Professor at the Universität Dortmund in June 1990. In 1995, he became a Full Professor at the Universität Karlsruhe (TH), Karlsruhe, Germany. Since 2001, he has been a Group Leader at the Institut für Nanotechnologie, Forschungszentrum Karlsruhe GmbH. Since 2001, he has been a

coordinator of the Karlsruhe Deutsche Forschungsgemeinschaft (DFG)-Center for Functional Nanostructures (CFN). His current research interests include different areas of photonics, such as nonlinear-optical spectroscopy, ultrafast spectroscopy, extreme nonlinear optics, near-field optical spectroscopy, photonic bandgap materials, and photonic metamaterials. Since 2005, he has been a Topical Editor of the *Journal of the Optical Society of America: B*.

Prof. Wegener received the Research Award of the Alfried Krupp von Bohlen und Halbach-Stiftung in 1993, the Teaching Award of the State of Baden-Württemberg in 1998, the DFG-Leibniz Award in 2000, the Descartes-Prize of the European Union in 2005, the Research Award of the State of Baden-Württemberg in 2005, and the Carl Zeiss Research Award in 2006. Since 2006, he has been a member of Leopoldina, the German Academy of Sciences. Since 2008, he has been a Hector Fellow and a Fellow of the Optical Society of America (OSA).